Infrared Physics & Technology 75 (2016) 107–116

Contents lists available at ScienceDirect

Infrared Physics & Technology

journal homepage: www.elsevier.com/locate/infrared

Iteratively reweighted unidirectional variational model for stripe non-uniformity correction

Yongzhong Huang [a], Cong He [b], Houzhang Fang [c,*], Xiaoping Wang [d]

[a] School of Mathematics and Statistics, Huazhong University of Science and Technology, Wuhan, Hubei 430074, PR China
[b] School of Mathematics and Statistics, Wuhan University, Wuhan, Hubei 430072, PR China
[c] National Laboratory of Radar Signal Processing, Xidian University, Xi'an, Shaanxi 710071, PR China
[d] Institute of Radar and Electronic Warfare, Equipment Academy of Air Force, Beijing 100085, PR China

HIGHLIGHTS

- The iteratively reweighted algorithm is used to optimize the UTV correction model.
- Derive a formula to automatically update the regularization parameter.
- The method works well on weak and strong stripe nonuniformity noise.

ARTICLE INFO

Article history:
Received 6 October 2015
Available online 25 January 2016

Keywords:
Iteratively reweighted least square (IRLS)
Unidirectional variational
Non-uniformity correction
Estimate regularization parameters

ABSTRACT

In this paper, we propose an adaptive unidirectional variational nonuniformity correction algorithm for fixed-pattern noise removal. The proposed algorithm is based on a unidirectional variational sparse model that makes use of unidirectional characteristics of stripe nonuniformity noise. The iteratively reweighted least squares (IRLS) technique is introduced to optimize the proposed correction model, which makes the proposed algorithm easy to implement with existing conjugate gradient method without introducing additional variables and parameters. Moreover, we derive a formula to automatically update the regularization parameter from the images. Comparative experimental results on real infrared images indicate that the proposed method can remove the stripe nonuniformity noise effectively while maintaining more useful image details.

© 2016 Published by Elsevier B.V.

1. Introduction

Infrared imaging systems are widely used in numerous applications such as infrared surveillance system [1], spectral-signature analysis, and night vision. The images acquired with an infrared imaging system are often degraded by the spatial nonuniformity in the output due to varying gains and offsets between detector channels. The spatial nonuniformity noise is also referred to as spatial fixed-pattern noise, which may be random, non-random or nonperiodic. This form of noise reduces the signal to noise ratio in the images, which further affects the performance of the infrared imaging system in the readout and severely limits the application of the resulting images, such as object detection, recognition, and classification. Thus, it is critical to apply a nonuniformity correction (NUC) technique to the changing detector responses before the subsequent image interpretation processes are performed.

To data, in the existing NUC methods, the reference-based nonuniformity correction (RBNUC) [2–4] and scene-based nonuniformity correction (SBNUC) methods [5–7] are two kinds of widely adopted methods for achieving higher-quality images. The one-point, two-point, and multi-point methods are the commonly employed reference-based NUC methods [8]. Compared to the RBNUC methods, the SBNUC approach does not use external references or calibration sources, but this kind of approach requires that the pixel values are varying between two adjacent frames images when sequences images are used. On the other hand, many NUC algorithms on the basis of a single image have received increasing attention for their effect and efficiency [9–13]. Munch et al. [9] utilized a Gaussian filter to filter the wavelet components in the Fourier domain, then the inverse Fourier transform is used to form the de-striped wavelet component at each level, and finally, the de-striped image can be reconstructed by inverse wavelet transform. Although their algorithm has achieved the impressive

* Corresponding author. Tel.: +86 29 88201400.
E-mail addresses: huangyz@hust.edu.cn (Y. Huang), joseph_hecong@126.com (C. He), houzhangfang@xidian.edu.cn (H. Fang), wangxiaoping_hs@163.com (X. Wang).

http://dx.doi.org/10.1016/j.infrared.2015.12.030
1350-4495/© 2016 Published by Elsevier B.V.

destriped results on nonperiodic striping patterns, the algorithm tends to introduce smear-like artifacts along the edges in the stripe direction. In addition, the algorithm needs to determine three parameters: the highest decomposition level L, the wavelet type, and the filtering threshold value for the Gaussian filter. Vera et al. [10] presented an adaptive SBNUC method based on minimization of isotropic total variation of the estimated irradiance to remove the fixed-pattern noise. Zhao et al. [12] proposed to convert the stripe NUC problem into a gradient-constrained optimization problem by keeping the vertical gradient close to the original image while minimizing the energy of the horizontal gradient. Tendero et al. [11] proposed a Midway Histogram Equalization (MHE) based single frame stripe noise correction algorithm. The main idea is to transport the histogram of each column to the midway of the histograms of the adjacent columns. This method does not requires a column time-dependent cross-calibration and test-pattern calibration. Thus, it is fully automatic and requires no user parameter. Recently, we also proposed a variational correction method [14] that combines unidirectional variation model and framelet regularization. It has already achieved the competitive destriping results. The rationality behind the proposed method in [14] lied in that unidirectional variation model based regularizations are effective for different kinds of stripe noise removal, and framelet regularization can well retain the detail information. Despite obtaining satisfactory results in the case of nonperiodic stripes patterns, the choice of the parameters for the approaches involved in [9,10,12,14] still need to address manually or heuristically in practical applications.

In this paper, we tackle the nonuniformity correction issue for the fixed-pattern noise as an inverse problem, i.e., from the given observed data to estimate the original scene. In fact, the nonuniformity correction problem is also an ill-posed inverse problem in most of real-world applications. Therefore, some a priori knowledge about the image and the noise must be adopted for constraining the space of candidate solutions. Obvious directional signature of the stripes noise for the remote sensing images has been demonstrated by several authors [15,14,16,17]. Clear directional signature of the stripes nonuniformity noise for the infrared images is also right. In terms of this simple observation, the unidirectional variation model has been widely utilized in fixed pattern noise removal [14,12] for its simpleness and efficiency. However, the optimization for the unidirectional variation based regularization models still has the room for improvement. On the other hand, the choice of the smoothing parameters in this kind of models is still not solved very well although it has significant effect on the result of correction process. The main ideas and contributions of the proposed approach are summarized as follows:

(i) The iteratively reweighted algorithm is introduced to optimize the proposed unidirectional variation non-uniformity correction model. The resulting optimization problem is converted into a least square problem, which is very easy to solve.
(ii) We derive a formula to automatically update the regularization parameter as the algorithm progresses.
(iii) The proposed method works well not only on weak stripe nonuniformity, but it also has the potential to remove strong stripe nonuniformity noise.

The remainder of this paper is organized as follows. In Section 2, we formulate the proposed model and the optimization algorithm. The experimental results and discussions are presented in Section 3. Section 4 presents our conclusions.

2. Formulation and algorithm

2.1. Problem formulation

We observe that stripe nonuniformity noise has obvious directional characteristics. Fig. 1 presents the derivatives of the stripe nonuniformity noise along horizontal and vertical directions of an infrared image. It is evidently seen that the horizontal direction

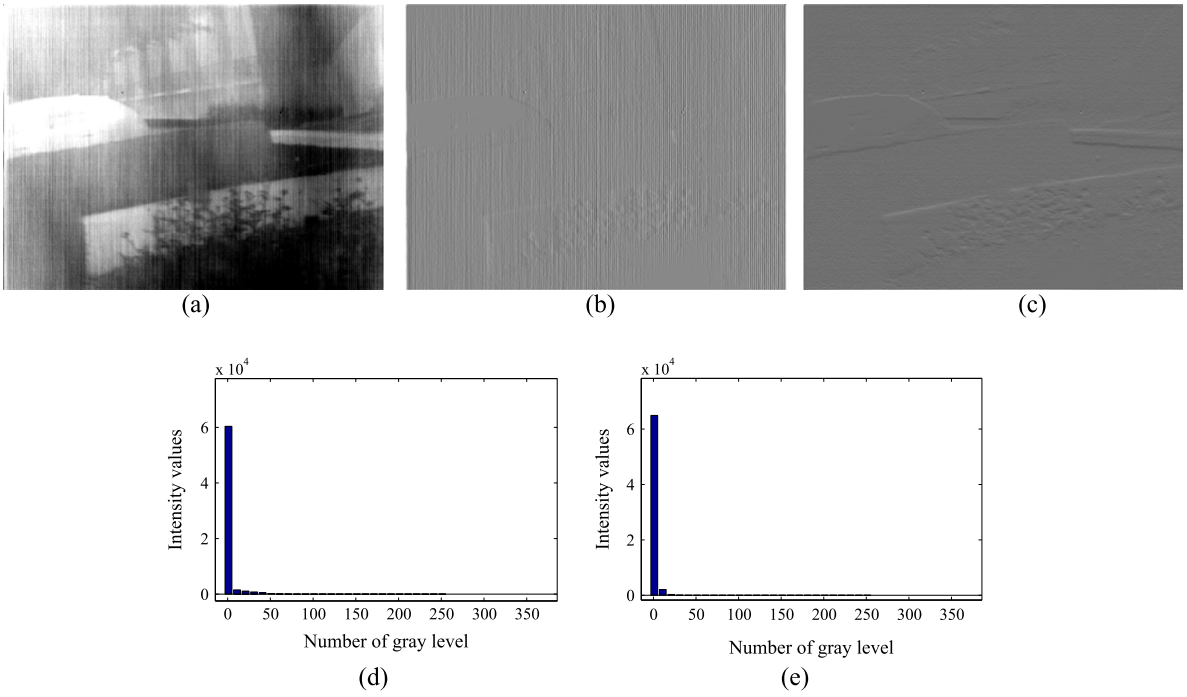


Fig. 1. (a) Stripe nonuniformity noise image (size: 288 × 384). (b) Horizontal direction gradient. (c) Vertical direction gradient. (d) Histogram of image (b). (e) Histogram of image (c).

gradient [Fig. 1(b)] includes the most stripe nonuniformity noise, while the vertical direction gradient [Fig. 1(c)] has hardly any stripe nonuniformity noise. Or in other words, the stripe nonuniformity leads to remarkable changes on gradient across the stripe noise lines, while it has few effects on the gradient along the stripe nonuniformity noise lines. Therefore, it is reasonable to retain the gradient along the stripe nonuniformity noise lines so as to preserve the image information while constraining the gradient across the stripe nonuniformity noise lines so as to eliminate the stripe nonuniformity. As shown in Fig. 1(d) and (e), we can also see that the histograms of the gradients of stripe nonuniformity noise image along horizontal and vertical directions are very sparse. Based on the observation and analysis mentioned above, we incorporate a unidirectional variational model into the optimization constraint framework

$$E(\mathbf{u}) = \frac{1}{p}\left\|D^{(2)}(\mathbf{u}-\mathbf{g})\right\|_p^p + \frac{\lambda}{q}\left\|D^{(1)}\mathbf{u}\right\|_q^q, \tag{1}$$

where $\mathbf{u}$ and $\mathbf{g}$ denote the latent and the observed images with the size of $n \times n$, respectively. $D^{(1)} \in \mathbb{R}^{n^2\times n^2}$ and $D^{(2)} \in \mathbb{R}^{n^2\times n^2}$ represent the two first-order forward finite difference operators under suitable boundary conditions along the horizontal and vertical directions, respectively. λ is the regularization parameter. $0 \leqslant p \leq 1$ and $0 \leqslant q \leq 1$ are the norm index, here $\|\mathbf{x}\|_p^p = \sum_{k=1}^n |x_i|^p$ for the vector $\mathbf{x} = \{x_1, x_2, \ldots, x_n\}^T, T$ represents the transpose operation. The unidirectional variational functional (1) is intuitive. The first term implies that we attempt to find an image that has almost the same vertical variation as the noisy one, which is very logical since the stripe nonuniformity noise mostly affects the horizontal direction. The aim of the second term is to penalize the ℓ_q-norm of the

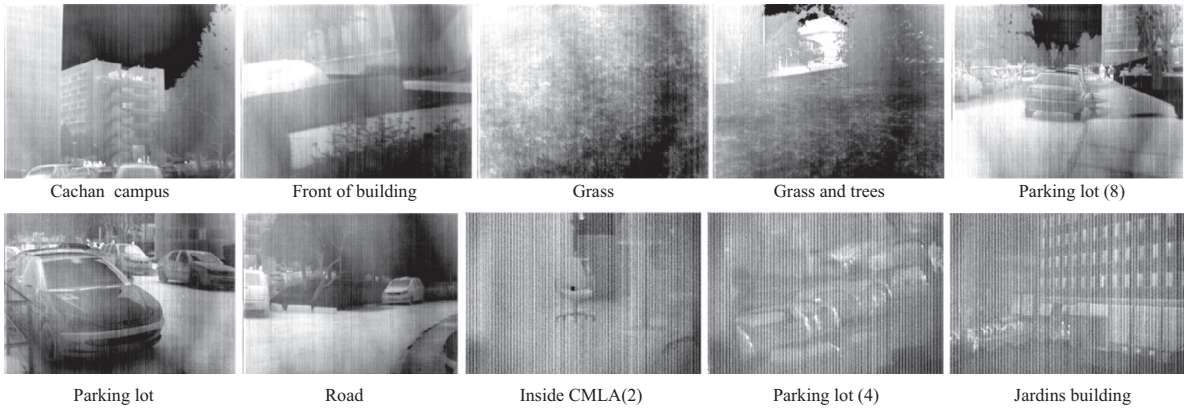


Fig. 2. Set of infrared images. First row (from left to right): Cachan campus, front of building, grass, grass and trees, and parking lot (8). Second row (from left to right): parking lot, road, inside CMLA, parking lot (4), and Jardins building.



Fig. 3. (a) The corrected result with the regularization parameter $\lambda = 0.005$ ($\rho = 0.12$). (b) The corrected result with the optimal estimating regularization value $\lambda = 0.0085$ ($\rho = 0.11$). (c) The corrected result with the regularization parameter $\lambda = 0.02$ ($\rho = 0.15$).

Table 1
Comparison of roughness index (ρ) and processing time (unit: second) for three methods.

Image	Image size	Observed (ρ)	Wavelet-FFT [9] (ρ/time)	MIRE [11] (ρ/time)	Proposed (ρ/time)
Cachan campus	288 × 384	0.19	0.12/0.44	0.13/1.89	0.10/2.28
Front of building	288 × 384	0.19	0.11/0.47	0.12/1.87	0.09/2.07
Grass	288 × 384	0.22	0.14/0.44	0.15/1.94	0.12/2.23
Grass and trees	288 × 384	0.24	0.18/0.43	0.18/1.87	0.15/1.90
Parking lot (8)	288 × 384	0.23	0.13/0.48	0.15/1.90	0.11/2.28
Parking lot	269 × 384	0.32	0.20/0.49	0.22/1.72	0.15/1.63
Road	288 × 384	0.22	0.13/0.53	0.15/1.90	0.11/2.07
Inside CMLA	220 × 320	0.94	0.37/0.44	0.33/1.20	0.29/0.74
Parking lot (4)	220 × 320	0.98	0.44/0.43	0.31/1.23	0.17/0.64
Jardins building	220 × 320	1.05	0.28/0.48	0.36/1.19	0.19/0.60

gradient across the stripe nonuniformity noise lines for correcting the stripe nonuniformity.

It is not an easy work to directly optimize the functional (1) due to the nonsmoothness and inseparableness of the ℓ_q-norm penalty (Similarly for ℓ_p norm). Some recent fast optimization methods, such as split Bregman technique [18,14] and alternative direction method of multipliers [19], can be used to convert the original problem (1) into several separate subminimization problems, which are easy to solve. However, these fast optimization techniques also introduce additional auxiliary variables and parameters. A large number of iterations have to be performed for achieving the satisfactory results. On the other hand, the iterative reweighted least squares (IRLS) algorithms have been proven that they are simple, flexible, and computational efficient [20,21]. In this research, we use IRLS algorithm for solving the unidirectional variational functional.

2.2. Numerical algorithm

The main idea of IRLS algorithm is to approximate unidirectional variational functional (1) by a weighted ℓ_2-norm form and update the solution and weight by an iterative scheme. Under the IRLS framework, the functional (1) can be written as follows:

$$J(\mathbf{u}) = \frac{1}{2}\left\|W_1^{1/2}\left(D^{(2)}(\mathbf{u}-\mathbf{g})\right)\right\|_2^2 + \frac{\lambda}{2}\left\|W_2^{1/2}D^{(1)}\mathbf{u}\right\|_2^2, \tag{2}$$

where

$$W_1 = \mathrm{diag}\left(\frac{2}{p}\phi\left(D^{(2)}(\mathbf{u}-\mathbf{g})\right)\right), W_2 = \mathrm{diag}\left(\frac{2}{q}\psi\left(D^{(1)}\mathbf{u}\right)\right). \tag{3}$$

Here, diag($\mathbf{x}$) denotes a diagonal matrix of the vector $\mathbf{x}$ and

$$\phi(x) = \begin{cases} |x|^{p-2}, & \text{if } |x| > \varepsilon_1, \\ \varepsilon_1^{p-2}, & \text{if } |x| \leqslant \varepsilon_1, \end{cases} \psi(x) = \begin{cases} |x|^{q-2}, & \text{if } |x| > \varepsilon_2, \\ \varepsilon_2^{q-2}, & \text{if } |x| \leqslant \varepsilon_2. \end{cases} \tag{4}$$

ε_1 and ε_2 are two small positive numbers. The functions $\phi(\cdot)$ and $\psi(\cdot)$ are defined to avoid division by zero-valued components.

The new functional (2) is a least-square problem, which is very easy to iteratively minimize. The gradient of the quadratic functional (2) can be easily derived as follows:

$$\left(D^{(2)}\right)^T W_1 D^{(2)}(\mathbf{u}-\mathbf{g}) + \lambda\left(D^{(1)}\right)^T W_2 D^{(1)}\mathbf{u} = 0. \tag{5}$$

2.3. Estimation of the unidirectional variational regularization parameter

We define a functional as follows

$$F(\mathbf{u};\lambda) = \sum_i \left(\left(D^{(2)}\right)^T W_1 D^{(2)}(\mathbf{u}-\mathbf{g}) + \lambda\left(D^{(1)}\right)^T W_2 D^{(1)}\mathbf{u}\right)^2, \tag{6}$$

which should obtain zero value when Eq. (5) is fulfilled. At the kth correction iteration, the regularization parameter λ can be chosen such that the functional $F(\mathbf{u}_k;\lambda)$ achieves its minimum. With current solution, let the derivative of the functional $F(\mathbf{u};\lambda)$ with respect to the parameter λ be zero, the updating formula of the optimal λ can be written as follows

$$\lambda_k = \frac{\sum_i \left(D^{(2)}\right)^T W_1 D^{(2)}(\mathbf{u}_k-\mathbf{g}) \cdot \left(D^{(1)}\right)^T W_2 D^{(1)}\mathbf{u}_k}{\sum_i \left(\left(D^{(1)}\right)^T W_2 D^{(1)}\mathbf{u}_k\right)^2}. \tag{7}$$

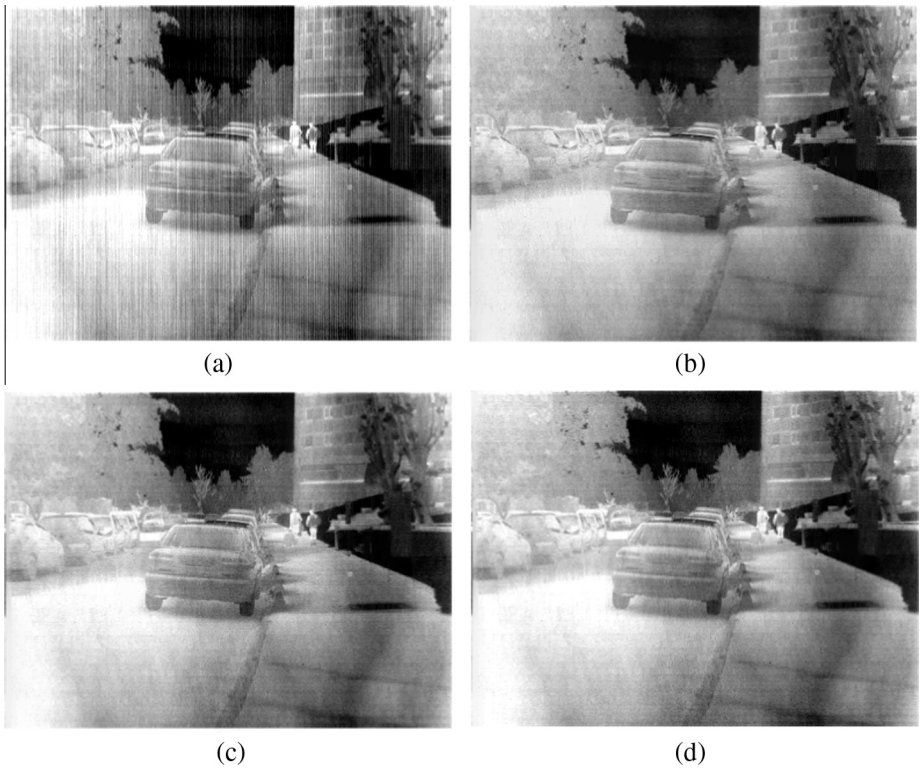


Fig. 4. The corrected results for three iterations. (a) Parking lot (8). (b) The corrected result in the first iteration ($\rho = 0.1123$). (c) The corrected result in the second iteration ($\rho = 0.1124$). (d) The corrected result in the third iteration ($\rho = 0.1125$).

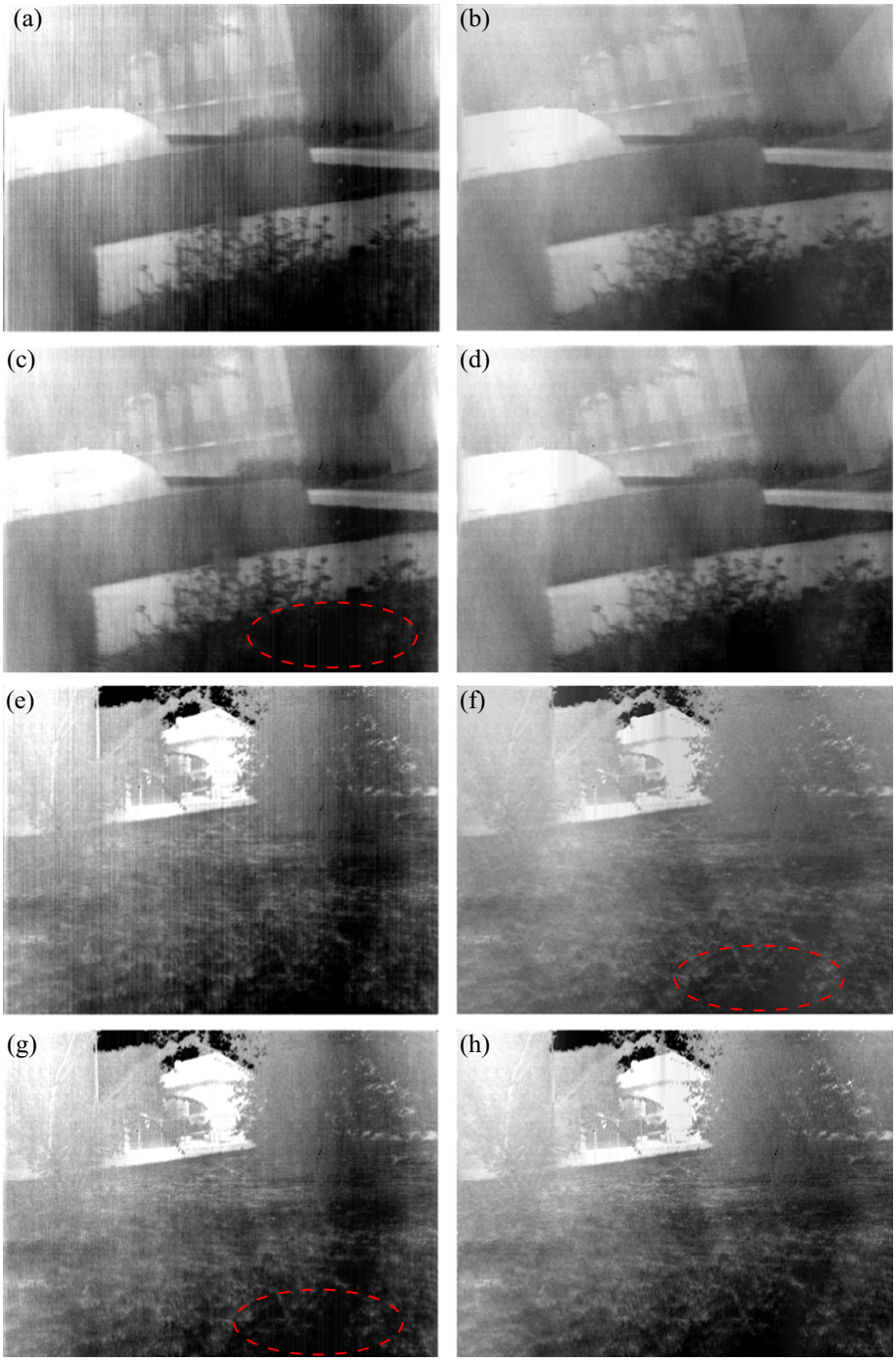


Fig. 5. Correction of partial infrared images. (a) and (e) are the front of building and grass and trees. (b), (f); (c), (g) and (d), (h) are the results obtained using wavelet-FFT [9], MIRE [11], and the proposed method, respectively.

Algorithm 1. IRLS algorithm for the unidirectional variational model

Input: Nonuniformity noisy image $\mathbf{g}$.
Initialization: $\mathbf{u}_0 = \mathbf{g}$. $\varepsilon_1 = 0.0001, \varepsilon_2 = 0.0001, \text{tol} = 0.0001$.
for $k = 0$ to K_{MaxIter} and $\|\mathbf{u}_k - \mathbf{u}_{k+1}\|_2 / \|\mathbf{u}_k\|_2 < \text{tol}$ **do**
  (1) Update the weight: $W_{1,k} = \text{diag}\left(\frac{2}{p}\phi(\nabla_y(\mathbf{u}_k - \mathbf{g}))\right)$;
  (2) Update the weight: $W_{2,k} = \text{diag}\left(\frac{2}{q}\psi(\nabla_x \mathbf{u}_k)\right)$;
  (3) Update the parameter λ_k according to (7);
  (4) Calculate the solution:

$$\mathbf{u}_{k+1} = \left(W_{2,k} + \lambda_k \left(D^{(1)}\right)^T W_{2,k} D^{(1)} + \lambda_k \left(D^{(2)}\right)^T W_{1,k} D^{(2)})^{-1} W_{2,k}\mathbf{g};$$

  (5) Update $k := k + 1$.
end for

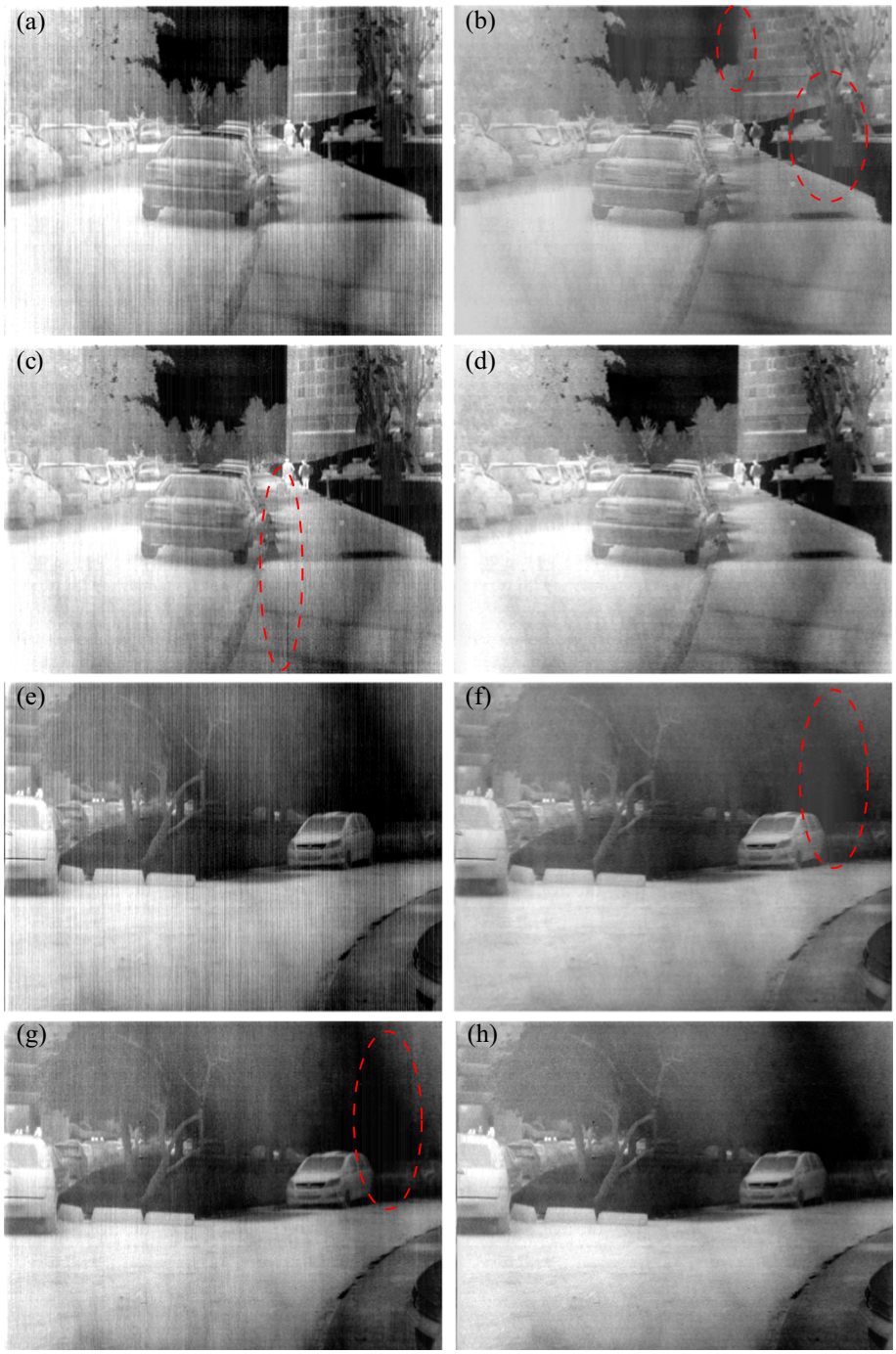


Fig. 6. Correction of three infrared images. (a) and (e) are the parking lot (8) and road. (b), (f); (c), (g) and (d), (h) are the results obtained using wavelet-FFT [9], MIRE [11], and the proposed method, respectively.

Taking into account the above equations, the complete algorithm is summarized in Algorithm 1.

It is impractical to directly compute the matrix inverse in line 8 of the Algorithm 1 for many cases. An alternative way is to compute the matrix inversion using the conjugate gradient (CG) method, which is much faster than computing the exact solution.

3. Experiments and discussion

In this section, we validate our proposed method in real images, which are from a publicly infrared image data set as shown in Fig. 2. The state-of-the-art wavelet-FFT filtering method (wavelet-FFT) in [9] and the tripe uniformity noise removal method (MIRE) in [11,22,23] are also performed for comparison. The input images are normalized between [0, 1]. The parameters in [9,23] are set based on the suggestions in their paper for the optimal performance. In Algorithm 1, both p and q can be set any real number between 0 and 1. However, we find that the algorithm does not produce significant superior results for $p \in (0,1)$ and $q \in (0,1)$ when compared with $p = 1$ and $q = 1$. Therefore, we set $p = 1$ and $q = 1$. Our method is performed in Matlab (R2013a) without parallel-computing implementation on a PC computer with an Intel Core i7-4770 CPU (3.40 GHz) and 8 GB memory.

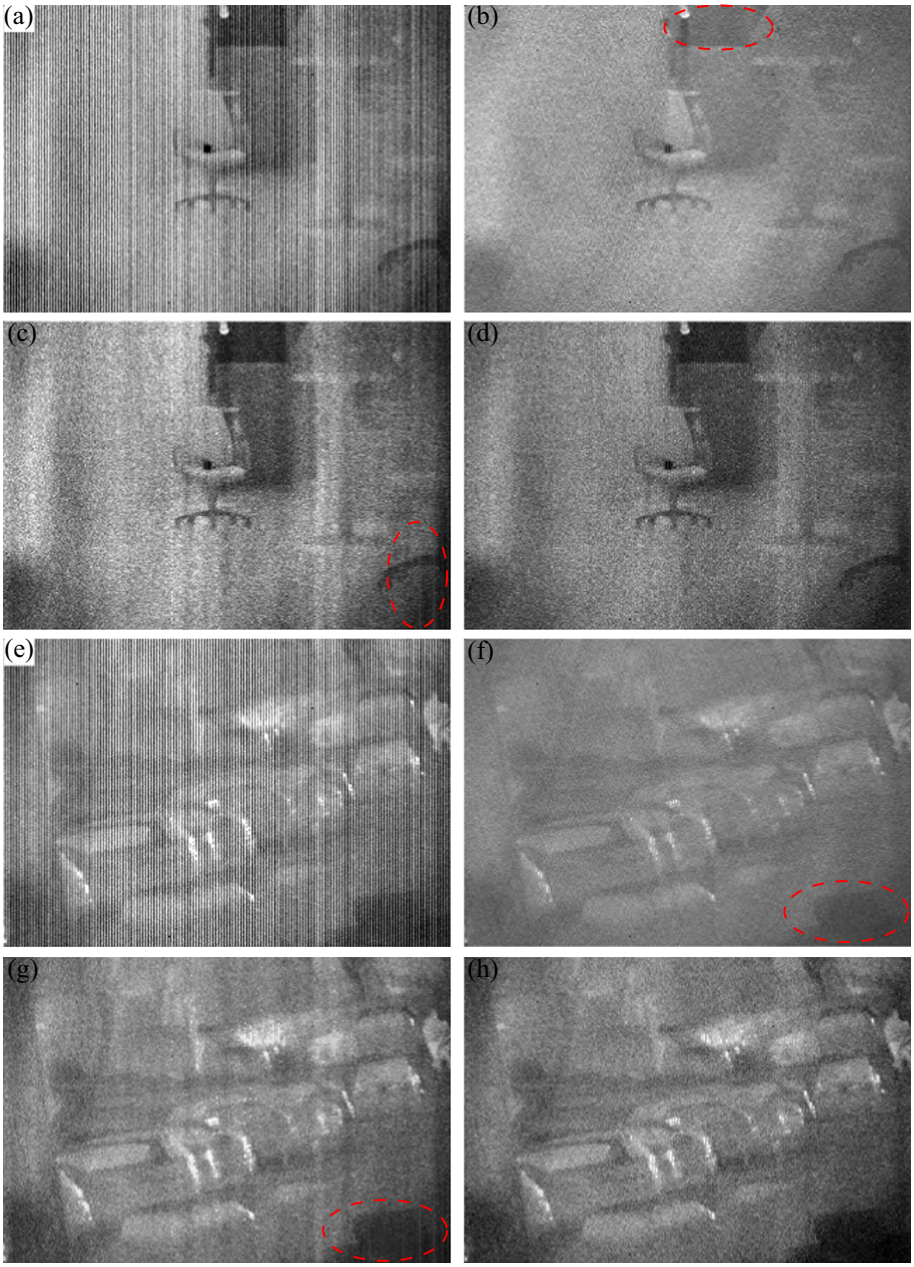


Fig. 7. Correction of three infrared images with severe stripe nonuniformity noises. (a) and (e) are the front of building and grass and trees. (b), (f); (c), (g) and (d), (h) are the results obtained using wavelet-FFT [9], MIRE [11], and the proposed method, respectively.

The NUC methods are evaluated through qualitative and quantitative assessments via visual inspection and a quantitative index. A reference-free metric so-called roughness index (ρ) is introduced to quantitatively evaluate the performance of NUC and calculated as follows:

$$\rho(\mathbf{u}) = \frac{\|h_1 * \mathbf{u}\|_2 + \|h_2 * \mathbf{u}\|_2}{\|\mathbf{u}\|_2}, \tag{8}$$

where h_1 and h_2 are the spatial filters $[1, -1]$ and $[1; -1]$, respectively. $\mathbf{u}$ is an image. $\|\mathbf{u}\|_2$ denotes the ℓ_2 norm of $\mathbf{u}$ (Euclidean norm) and $*$ denotes the discrete two dimension convolution. For the roughness index, the smaller the ρ is, the better the algorithm performance.

3.1. Validation of the effectiveness of adaptively estimating regularization parameter

The nonuniformity correction algorithm with unidirectional variational regularization has been shown to present good correction results with an appropriately chosen regularization parameter λ. In the following, we present the experiments to compare the results with the parameters which are estimated from the images with the results with the manually selected parameters. Fig. 3(a), (c), and (b) are the corrected results with the manually selected regularization parameters $\lambda = 0.005$ ($\rho = 0.12$), $\lambda = 0.02$ ($\rho = 0.15$), and the estimated value $\lambda = 0.0085$ ($\rho = 0.11$) using the formula (7), respectively. From the comparison of the corrected images, we can see that the results with smaller and bigger regularization parameters have higher roughness indexes compared to the result using the adaptively estimated parameter. Small

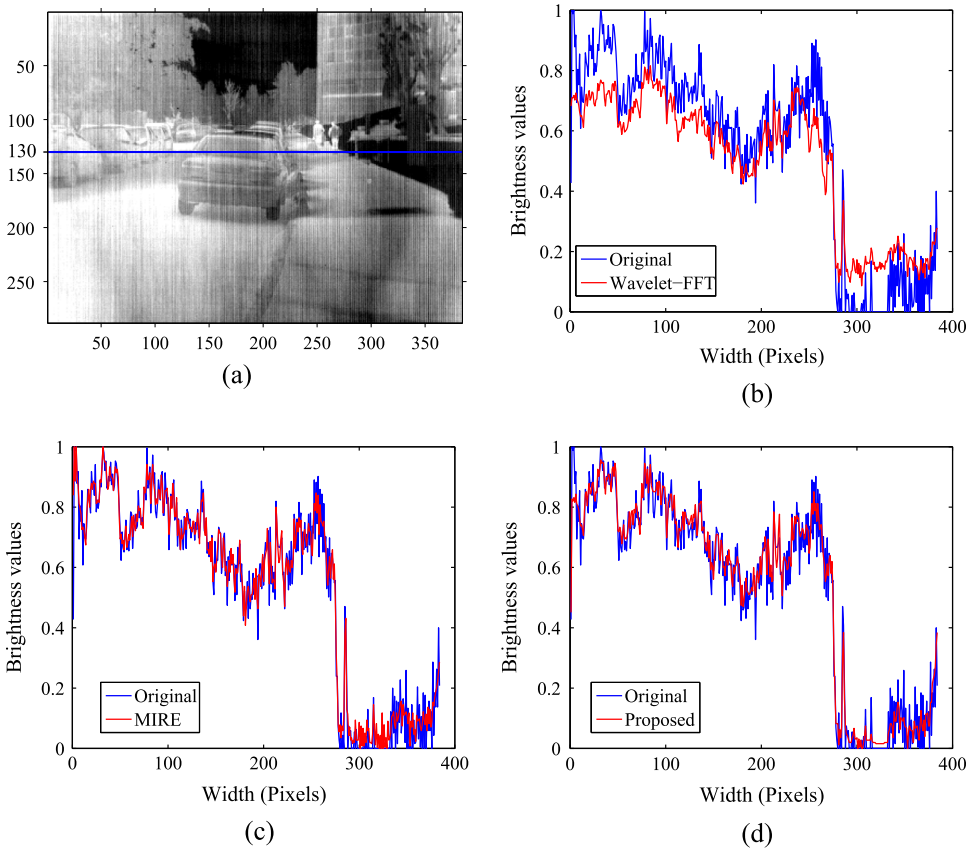


Fig. 8. Profiles of the corrected images shown in Fig. 6(b)–(d) at row 130. (a) Original parking lot (8). (b) Wavelet-FFT. (c) MIRE. (d) Proposed method. (Original in blue and corrected in red.) (For interpretation of the references to colour in this figure legend, the reader is referred to the web version of this article.)

regularization parameter will lead to residual stripes and large regularization parameter will cause over smoothing of image. Thus, the proposed algorithm is advantage to correcting stripe nonuniformity noise by using an appropriately estimated regularization parameter depending on the input image.

3.2. Real experiments

Table 1 lists the roughness index and processing time for three methods. From the Table 1, we can find that the proposed method obtains a relatively lower roughness index for each image. This implies that the proposed method obtains the better performance compared to other two methods. As for the computational time, the MIRE method takes the less time to reach the convergence at most of the cases compared to the proposed method, while the wavelet-FFT filter method's execution time is the least among three methods.

Fig. 4 shows the corrected results from three iterations for the image Parking lot(8). In the Algorithm 1, we find that it takes about two outer iterations to converge to a satisfactory result. The algorithm does not provide significantly superior results when the number of iterations is larger than two. So, in the Algorithm 1, we set $K_{\mathrm{MaxIter}} = 3$.

For visual perception of the final corrected results by the wavelet-FFT [9] method, the MIRE [11] method, and the proposed approach, Figs. 5 and 6 presents the corrected images of four infrared images from the Fig. 2. In Figs. 5(b), (f) and 6(b), (f), although most of the stripe nonuniformity noises are eliminated by the wavelet-FFT filter method, some detail information that belongs to the image itself is also weakened along with the removal of the stripe nonuniformity, which degrades the image contrast. In Figs. 5(c), (g) and 6(c), (g), the MIRE [11] method removes most of the stripe noncuniformity noise, but some residual nonuniformity noises still can be clearly seen in the dark areas. In Figs. 5 (d), (h) and 6(d), (h), the stripe nonuniformity noise are completely removed by the proposed method, and the detail information can be preserved well. Overall, compared to the wavelet-FFT and MIRE methods, the proposed method performs consistently over four infrared images and the corrected results are of good quality with satisfactory visual quality.

To further validate the ability of the proposed approach, we perform our method on two severe stripe nonuniformity noise images. As shown in Fig. 7(a) and (e), the image details are almost covered up by severe stripe nonuniformity noise. In Fig. 7(b) and (f), we can observe that the wavelet-FFT filter method does not perform well on images with severe stripe nonuniformity noise. Most of stripe nonuniformity noise are removed, but the results also present obvious oversmoothing effect, which leads to detail information loss in the dark and edges regions. From Fig. 7(c) and (g), residual nonuniformity noise still can be observed in the homogeneous areas as marked from red circle. In Fig. 7(d) and (h), the severe stripes nonuniformity are well removed with fewer artifacts. The proposed method is better than the wavelet-FFT and MIRE methods in terms of minimal distortions and preserving details. The superior performance of the proposed method on the severe stripe nonuniformity noise images demonstrates that the potential of the method for practical application on severe stripe noise images.

The profiles shown in Fig. 8 denotes the profiles perpendicular to the striping direction (along row 130). By comparing these horizontal profiles before and after correction, we can find that the image profiles achieved by three methods are more smoother than that of the original. These profiles indicate that the proposed

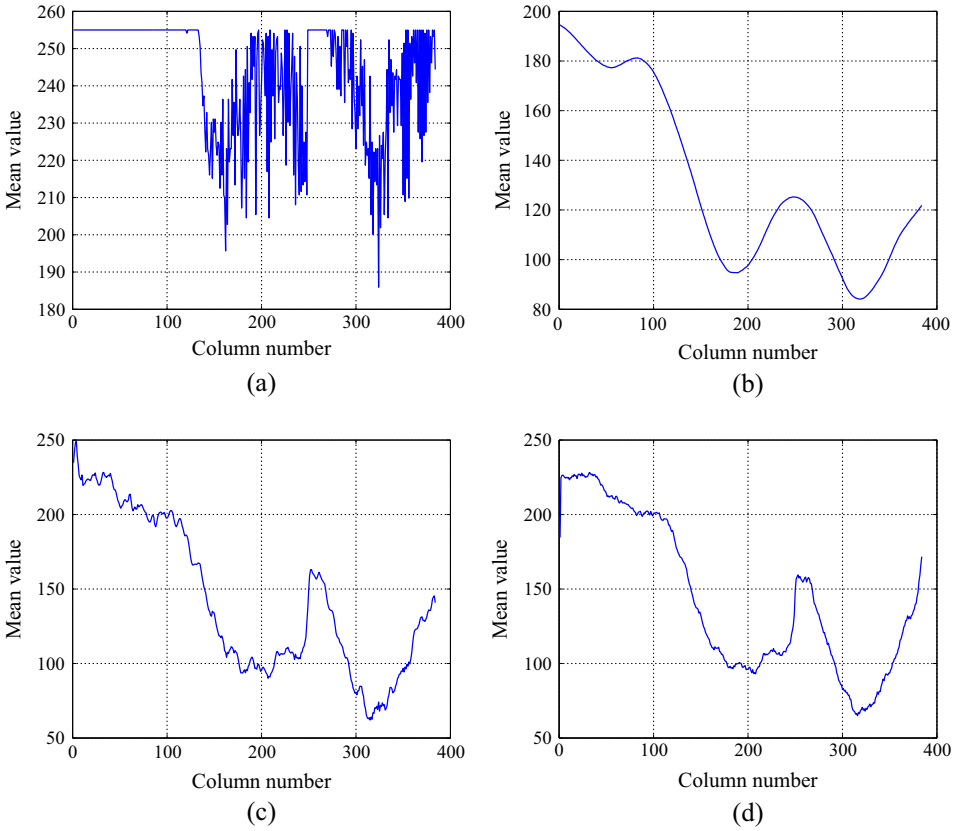


Fig. 9. Mean cross-track profiles for images shown in Fig. 6(a)–(d). (a) Original parking lot (8). (b) Wavelet-FFT. (c) MIRE. (d) Proposed method.

method is superior in removing the stripe nonuniformity noise while preserving the useful content of the original image.

Fig. 9 displays the mean cross-track profiles before and after correction. The horizontal axis and the vertical axis represent the column number and the mean value of each column, respectively. Due to the presence of the stripe nonuniformity noise, the mean cross-track profile of the original image fluctuates wildly as shown in Fig. 9(a). In Fig. 9(b), the mean cross-track profile is oversmoothing, this means that the details from the original images are significantly reduced. There are still some burrs in the Fig. 9(c). This illustrates some residual stripes still exist in the correction result (Fig. 6(c)). Fig. 9(d) is the profile of the corrected image achieved by the proposed method, which provides a relatively smooth curve. This again validates that the ability of the proposed algorithm in eliminating the stripe noise while maintaining the detail information of the original data.

3.3. Limitation

In our correction Algorithm 1, classical conjugate gradient method is still not very efficient, which takes up most of the Algorithm 1. In the future, we would like to introduce an accelerated technique by invoking the preconditioned conjugate gradient method [24] to reduce the computational cost.

In our proposed model, both p and q can equal to zero. However, we do not discuss this situation in our paper. In the future, we will further investigate this situation in detail.

4. Conclusion

In this paper, a new NUC correction algorithm is presented to remove stripe nonuniformity noise from a single image based on the unidirectional variational model. Moreover, iteratively reweighted technique is exploited to convert the unidirectional variational correction model into a least square problem. In addition, we have derived a formula to automatically estimate the regularization parameter for the unidirectional variational correction algorithm. Hence, the proposed method is more robust with the choice of the regularization parameter, which makes it very attractive for practical applications.

Conflicts of interest

The authors declare that there is no conflict of interests regarding the publication of this article.

Acknowledgments

This work was supported by the National Natural Science Foundation of China under Grant 41501371 and "Fundamental Research Funds for the Central Universities" under Grant XJS15004.

References

[1] J. Hu, Z. Xu, Q. Wan, Non-uniformity correction of infrared focal plane array in point target surveillance systems, Infrared Phys. Technol. 66 (2014) 56–59.
[2] M. Schultz, L. Caldwell, Nonuniformity correction and correctability of infrared focal plane arrays, Infrared Phys. Technol. 36 (4) (1995) 763–777.
[3] R. Wang, P. Chen, P. Tsien, An improved nonuniformity correction algorithm for infrared focal plane arrays which is easy to implement, Infrared Phys. Technol. 39 (1) (1997) 15–21.
[4] Z. Cai, Y. Shi, T. Zhang, L. Hui, A feasible approach for nonuniformity correction in irfpa with nonlinear response, Infrared Phys. Technol. 46 (4) (2005) 460–489.
[5] J. Zhao, X. Gao, Y. Chen, H. Feng, Z. Xu, Q. Li, Fast iterative adaptive nonuniformity correction with gradient minimization for infrared focal plane arrays, Infrared Phys. Technol. 65 (2014) 87–93.

[6] C. Zuo, Y. Zhang, Q. Chen, G. Gu, W. Qian, X. Sui, J. Ren, A two-frame approach for scene-based nonuniformity correction in array sensors, Infrared Phys. Technol. 60 (2013) 190–196.
[7] W. Qian, Q. Chen, J. Bai, G. Gu, Adaptive convergence nonuniformity correction algorithm, Appl. Opt. 50 (2010) 1–10.
[8] S. Kim, Two-point correction and minimum filter-based nonuniformity correction for scan-based aerial infrared cameras, Opt. Eng. 51 (10) (2012). 106401(1–13).
[9] B. Münch, P. Trtik, F. Marone, M. Stampanoni, Stripe and ring artifact removal with combined wavelet-Fourier filtering, Opt. Express 17 (10) (2009) 8567–8591.
[10] E. Vera, P. Meza, S. Torres, Total variation approach for adaptive nonuniformity correction in focal-plane arrays, Opt. Lett. 36 (2) (2011) 172–174.
[11] Y. Tendero, J. Gilles, S. Landeau, J.M. Morel, Efficient single image non-uniformity correction algorithm, in: Society of Photo-Optical Instrumentation Engineers (SPIE) Conference Series, vol. 7834, 2010, pp. 1–10.
[12] J. Zhao, Q. Zhou, Y. Chen, T. Liu, H. Feng, Z. Xu, Q. Li, Single image stripe nonuniformity correction with gradient-constrained optimization model for infrared focal plane arrays, Opt. Commun. 296 (1) (2013) 47–52.
[13] Y. Cao, Y. Li, Strip non-uniformity correction in uncooled long-wave infrared focal plane array based on noise source characterization, Opt. Commun. 339 (2015) 236–242.
[14] Y. Chang, H. Fang, L. Yan, H. Liu, Robust destriping method with unidirectional total variation and framelet regularization, Opt. Express 21 (20) (2013) 23307–23323.
[15] M. Bouali, S. Ladjal, Toward optimal destriping of modis data using a unidirectional variational model, IEEE Trans. Geosci. Remote Sens. 49 (8) (2011) 2924–2935.
[16] G. Zhou, H. Fang, L. Yan, T. Zhang, J. Hu, Removal of stripe noise with spatially adaptive unidirectional total variation, Optik 125 (12) (2014) 2756–2762.
[17] G. Zhou, H. Fang, C. Lu, S. Wang, Z. Zuo, J. Hu, Robust destriping of MODIS and hyperspectral data using a hybridunidirectional total variation model, Optik 126 (7–8) (2015) 838–845.
[18] T. Goldstein, S. Osher, The split Bregman method for L1-regularized problems, SIAM J. Imaging Sci. 2 (2009) 323–343.
[19] S. Boyd, N. Parikh, E. Chu, B. Peleato, J. Eckstein, Distributed optimization and statistical learning via the alternating direction method of multipliers, Found. Trends Machine Learn. 3 (2011) 1–122.
[20] I. Daubechies, R. DeVore, M. Fornasier, S. Gunturk, Iteratively reweighted least squares minimization for sparse recovery, Commun. Pur. Appl. Math. 63 (2010) 1–38.
[21] P. Rodriguez, B. Wohlberg, Efficient minimization method for a generalized total variation functional, IEEE Trans. Image Process. 18 (2009) 322–332.
[22] J. Delon, Midway image equalization, J. Math. Imaging Vis. 21 (2012) 119–134.
[23] Y. Tendero, S. Landeau, J. Gilles, Non-uniformity correction of infrared images by midway equalization, Image Process. On Line (2012) 1–12.
[24] C. Chen, J. Huang, L. He, H. Li, Preconditioning for accelerated iteratively reweighted least squares in structured sparsity reconstruction, in: Proc. IEEE Conf. Computer Vision and Pattern Recognition, 2014, pp. 2713–2720.